Bulk Polymerization of Styrene in the Presence of Organomodified Montmorillonite

Guodong Liu, Liucheng Zhang, Dongmei Zhao, Xiongwei Qu

Institute of Polymer Science and Engineering, School of Chemical Engineering, Hebei University of Technology, Tianjin, 300130, People's Republic of China

Received 10 May 2004; accepted 21 October 2004
DOI 10.1002/app.21559
Published online in Wiley InterScience (www.interscience.wiley.com).

ABSTRACT: The effect of montmorillonite (Cloisite 6A) on the bulk polymerization of styrene initiated by benzoyl peroxide (BPO) was studied by the dilatometric determination of the polymerization rates. The bulk polymerization rates increased as the montmorillonite input quantity increased. The effect became greater when the BPO concentration decreased. Under the assumption that clay participated in the radical initiation reaction of the chains, the reaction orders for clay and BPO were determined to be approximately 1.0 and 0.5, respectively. X-ray diffraction and thermogravimetric analysis studies showed that the structure and properties of the obtained polystyrene (PS)/montmorillonite nanocomposites were greatly affected by the BPO concentration. With lower BPO concentrations, a larger interlayer distance and a higher extent of delamination for the clay were observed in the obtained PS/montmorillonite nanocomposites. The nanocomposites prepared with lower BPO concentrations also showed higher heat-decomposition-resistance temperatures. © 2005 Wiley Periodicals, Inc. J Appl Polym Sci 96: 1146–1152, 2005

Key words: clay; kinetics (polym.); nanocomposites; polystyrene; radical polymerization

INTRODUCTION

Clays have been used widely for the preparation of polymer/clay nanocomposites (PCNs). In recent years, much attention has been paid to PCNs as advanced plastic materials prepared via *in situ* intercalative polymerization, and montmorillonite (MMT) is the most widely used clay.[1] Intercalative compounding by bulk, solution, suspension, and emulsion polymerization have been studied widely. Most studies have focused on the changes in the layer structures of MMT caused by the usage of intercalative agents with different structures and compounding by different intercalative polymerization methods.

The uses of clay as a solid acid catalyst and the utility of clay-supported reagents were described in 1970s. Since then, there have been many reports on the catalytic activation of clay-based materials involving a tremendous variety of organic reactions.[2]

Uskov[3] reported that methyl methacrylate (MMA) could graft onto air-dry sodium bentonite under vibrodisintegration. The results showed that bentonite had an initiation effect on the polymerization of vinyl monomers. The emulsion polymerization of MMA in the presence of MMT was studied by Al-Esaimi,[4] and the results showed that the polymerization rate of MMA with potassium persulfate as the initiator increased in the presence of MMT. The catalytic effect of clay on the polymerization of MMA was attributed to the formation of a clay/$K_2S_2O_8$ complex, which accelerated the polymerization process. In a previous article,[5] we studied the bulk polymerization of MMA initiated by benzoyl peroxide (BPO) in the presence of organomodified montmorillonite (OMMT). The bulk polymerization rate of MMA increased with an optimal ratio of the OMMT content to the BPO concentration. Meanwhile, the layer structure of the obtained poly(methyl methacrylate) (PMMA)/OMMT nanocomposites was greatly affected by the BPO concentration. Obviously, the final properties of the obtained nanocomposites were also affected by the kinetics of the polymerization of the monomers.

However, a description of the effect of clay on polymerizations has been lacking until now. The aim of this work was to investigate the bulk polymerization of styrene (St) in the presence of clay (Cloisite 6A). Polymerization rates with different concentrations of an initiator (BPO) with or without the clay were determined. The activation energy (E_a) of the polymerization of St and the structure of the obtained polystyrene (PS)/Cloisite 6A nanocomposites were investigated.

EXPERIMENTAL

Materials

OMMT (Cloisite 6A, Southern Clay Products, Inc., Gonzales, TX) was used as received. Cloisite 6A was

Correspondence to: L. Zhang (gdliu@263.net).
Contract grant sponsor: National Science Foundation of Hebei Province; contract grant numbers: 202018 and 201006.

prepared by the ion exchange of sodium montmorillonite with dimethyl dehydrogenated tallow alkyl ammonium; the tallow was composed predominantly of octadecyl chains with small amounts of lower homologues. St (Tianjin Chemical Co., Tianjin, China) was analytically pure and was washed free of inhibitor with an aqueous solution of sodium hydroxide; it was then washed with deionized water, dried, and distilled twice under reduced pressure, with the middle fraction collected. BPO was an analytical reagent and was recrystallized twice in toluene before use.

Determination of the polymerization rates

The clay (Cloisite 6A) was dried *in vacuo* at 60°C for 24 h. All the glass vessels were washed with a potassium dichromate/concentrated sulfuric acid solution and distilled water and were dried before use.

Measured amounts of Cloisite 6A were impregnated in St in a triangular flask for 24 h. Then, accurately weighed BPO was added to the solution, and the system was ultrasonicated at 25°C for 10 min. The polymerization rates were measured dilatometrically in a water bath fixed at 60 ± 0.1°C. During the course of the reaction, no visible sediment was observed, and this indicated that it was a homogeneous system. After a preset time, the contents of the dilatometer were poured into a large amount of ethanol, and the products were isolated by filtration and then dried in an oven under reduced pressure to obtain a constant weight.

Instrumentation

Measurements of the average molecular masses and polydispersity indices (PDIs) of the polymers extracted and recovered from the composites were carried out with a Waters 51S-2410 gel permeation chromatography (GPC) apparatus (Milford, MA). Tetrahydrofuran was used as the flowing phase.

X-ray diffraction (XRD) patterns were recorded by the monitoring of the diffraction angle (2θ) from 1 to 15° on a DMAX-RC X-ray crystallographic unit. The unit was equipped with a Ni-filtered Cu Kα radiation (λ = 0.154 nm) source at a voltage of 50 kV and at a current of 180 mA. The scanning speed and step size were 1°/min and 0.02°, respectively.

Thermogravimetric analysis was carried out with a TA-2000 SDT2960 thermogravimetry instrument (TA Instruments, New Castle, DE) in an atmosphere of N_2 at a flow rate of 50 mL/min and a heating rate of 10°/min. The maximum-weight-loss-rate temperature (T_{max}) was used to evaluate the heat-decomposition resistance of the nanocomposites.

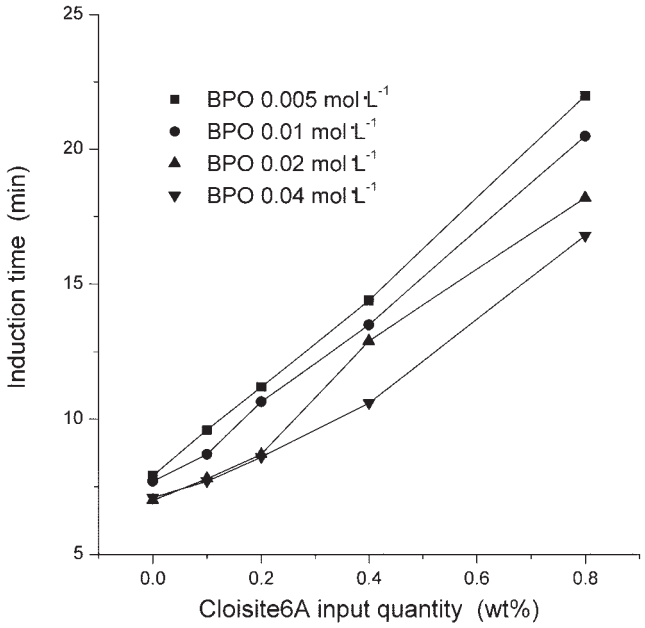

Figure 1 Effect of the input quantity of Cloisite 6A on the induction period of the bulk polymerization of St.

RESULTS AND DISCUSSION

Polymerization rates

The induction periods of the bulk polymerization of St are shown in Figure 1. The polymerization was postponed by the addition of MMT Cloisite 6A. This result was consistent with the early study of Solomon and Swift[6] on the polymerization of MMA initiated by BPO. This may have been due to the impurities in the clay or the aluminum on the crystal edges, which reacted with the primary radical. More clay contained more active spots, so the induction time was prolonged with increasing Cloisite 6A content.

The thermally initiated bulk polymerization rate of St was determined dilatometrically at 60°C with no BPO and clay added; it was determined to be 3.33 $\times 10^{-6}$ mol $L^{-1} \cdot s^{-1}$. Then BPO-initiated polymerization rates were calculated to eliminate the thermal initiation part as follows:

$$R_p^2 = R_{p0}^2 - R_{pT}^2 \quad (1)$$

where R_p and R_{pT} are the polymerization rates initiated by the initiator and heat, respectively, and R_{p0} is the overall polymerization rate. The relative ratios of the polymerization rates in the presence (R_p) and absence (R_{pI}) of Cloisite 6A are shown in Figure 2. R_p increased monotonically with increasing Cloisite 6A input quantity in the range of studied BPO concentrations. Figure 2 also indicates that when the Cloisite 6A input quantity increased, the difference between the relative increases of R_p at different BPO concentrations became larger. Obviously, the presence of clay increased the bulk polymerization rate of St.

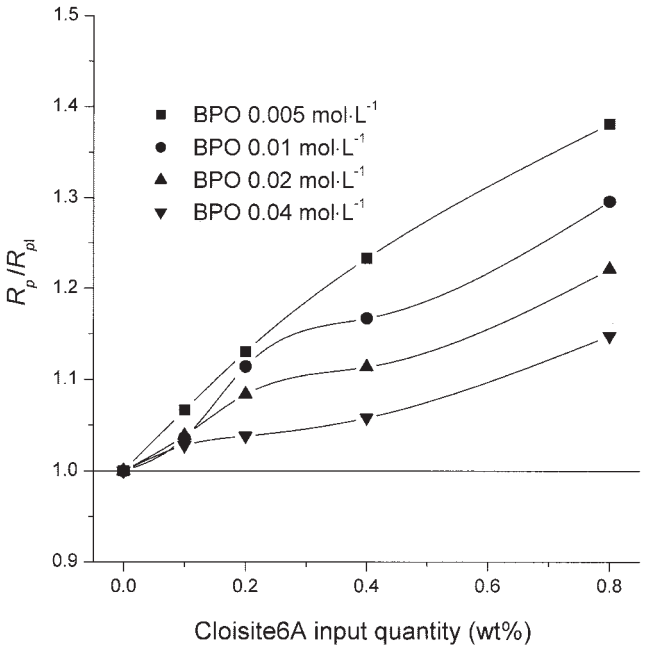

Figure 2 Relative ratio of the polymerization rates (R_p/R_{p0}) in the presence and absence of Cloisite 6A.

The increase in the polymerization rate could be attributed to the promotion of the clay on the chain initiation.[4] This seemed to contradict the postponement of the polymerization, but a further inspection could eliminate this suspicion. The extension of the induction period could be attributed to the impurities in the clay mineral, which was at a very low concentration. Its activity vanished after the induction period. The monotonic increase in R_p was different from that of the bulk polymerization of MMA in the presence of MMT in our previous article.[5] This was mostly because the activity of the MMA radical was 10 times higher than that of the St radical,[7] and so an increase in the concentration of the MMA radical could also increase the termination rate of the chain.

The classic radical polymerization theory provides the following equation:[7]

$$R_p = k[\mathrm{M}]^m[\mathrm{I}]^n \tag{2}$$

where [M] and [I] represent the concentrations of the monomer and initiator, respectively; m and n represent the reaction orders with respect to the monomer and initiator, respectively; and k is a general rate constant. The following equation was used to calculate n:

$$\ln R_p = \ln k + m \ln[\mathrm{M}] + n \ln[\mathrm{I}] \tag{3}$$

Because [M] was almost unchanged in the early stage of bulk polymerization, the slopes of the plots of ln R_p versus ln[I] shown in Figure 3 provide the n values, which are listed in Table I.

Table I shows that n was about 0.5 for the bulk polymerization of pure St, which indicated a bimolecular termination process.[8] n decreased with increasing Cloisite 6A input quantity, and this showed that the effect of BPO on the polymerization decreased. The results indicated that eq. (1) could not describe the bulk polymerization of St in the presence of MMT properly.

Kinetic investigation

To explain the increase in R_p, the bulk polymerizations of St at 50, 55, 60, and 65°C with 0.4 wt % Cloisite 6A and without clay were carried out. The BPO concentration was fixed at 0.005 mol L^{-1}. The results are shown in Figure 4. The E_a values were determined to be 91.71 and 81.74 kJ mol^{-1} without and with clay, respectively, with the Arrhenius equation as follows:

$$\ln R_p = \ln A - \frac{E_a}{R}\frac{1}{T} \tag{4}$$

where R_p is the initial polymerization rate at temperature T, A is the pre-exponential factor, and R is the gas constant. The obvious reduction of E_a was mainly due to the fact that the initiator and clay formed a complex[4] that accelerated the chain initiation of the polymerization. Unfortunately, the mechanism is not clear and requires a thorough study.

Therefore, the initiation of the chain was assumed to be composed of two reactions:

$$\mathrm{I} \xrightarrow{k_{d1}} \mathrm{R}\cdot \tag{5}$$

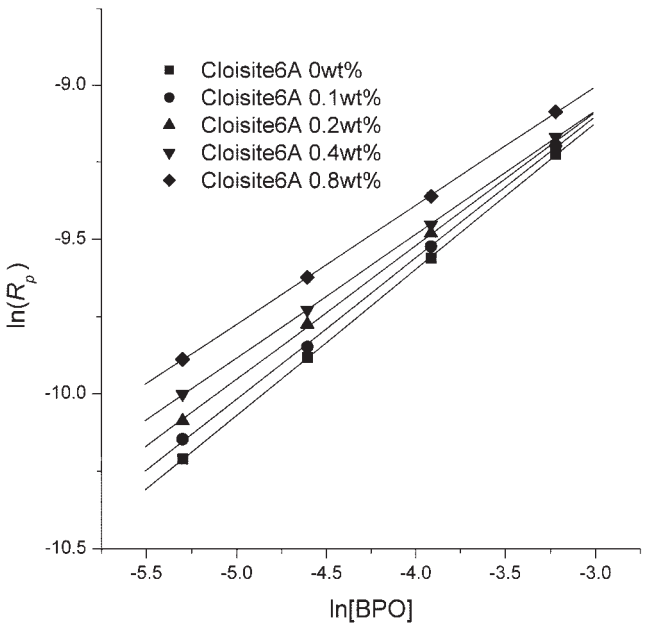

Figure 3 Plots of ln R_p versus ln[BPO].

TABLE I
Reaction Order (n) of the Bulk Polymerization of St with Respect to the BPO Concentration with Different Cloisite 6A Input Quantities

	Cloisite 6A input quantity (wt %)				
	0	0.1	0.2	0.4	0.8
n	0.473 ± 0.003	0.458 ± 0.006	0.432 ± 0.005	0.400 ± 0.002	0.384 ± 0.002

$$\mathrm{I} + \mathrm{C} \xrightarrow{k_{d2}} \mathrm{R}\cdot \tag{6}$$

where C represents Cloisite 6A, k_{d1} is the rate constant of initiator decomposition, and k_{d2} is the rate constant of the synergetic initiation of the initiator with clay. R_{iI} and R_{iIC} represent the initiation rates of reactions (5) and (6), respectively:

$$R_{iI} = f_1 k_{d1} [\mathrm{I}] \tag{7}$$

$$R_{iIC} = f_2 k_{d2} [\mathrm{I}]^{n_1} [\mathrm{C}]^{n_2} \tag{8}$$

where f_1 and f_2 are the initiation efficiencies of reactions (5) and (6), respectively; n_1 and n_2 are the orders of the reaction with respect to the initiator and clay, respectively; [I] is the initiator concentration; and [C] is the clay input quantity, which is proportional to the active spots on the clay sheets. Using the steady-state hypothesis and assuming a bimolecular termination process, we obtained the following:

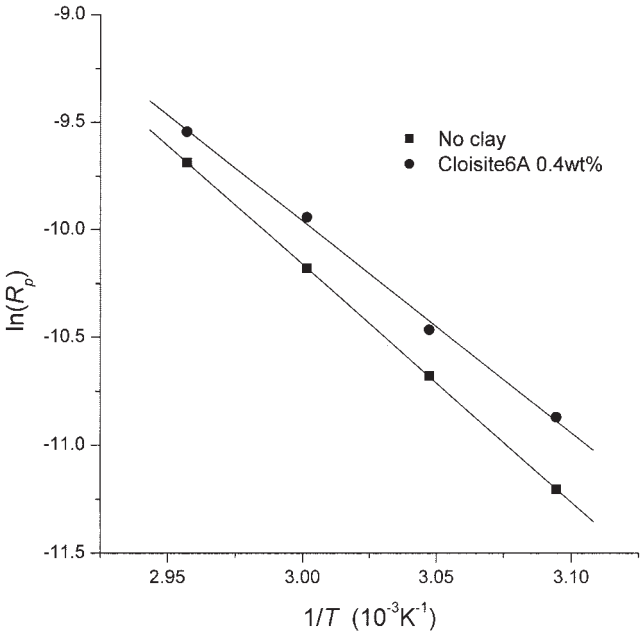

Figure 4 Bulk polymerization rates of St at different temperatures.

$$R_p^2 = \frac{k_p^{\,2}}{k_t} [\mathrm{M}]^2 (R_{iI} + R_{iIC}) \tag{9}$$

where k_p is the rate constant of chain propagation and k_t is the termination rate constant. If

$$R_{pI}^2 = \frac{k_p^2}{k_t} [\mathrm{M}]^2 R_{iI}$$

$$R_{pIC}^2 = \frac{k_p^2}{k_t} [\mathrm{M}]^2 R_{iIC}$$

where R_{pI} represents the polymerization rate without clay and R_{pIC} represents the rate of the polymerization initiated with the clay/BPO complex, then

$$R_{pIC}^2 = R_p^2 - R_{pI}^2 \tag{10}$$

$$R_{iIC} = \frac{k_t}{k_p^2 [\mathrm{M}]^2} R_{pIC}^2 \tag{11}$$

The linear fitting of ln R_{pIC}^2 with ln[BPO] and ln[C] provided the reaction orders of reaction (6) with respect to BPO and clay, respectively. The fitting results are presented in Figures 5 and 6 and yield $n_1 \approx 0.5$ and $n_2 \approx 1.0$. Then, the relative ratio of polymerization in the presence of clay can be described as follows:

$$\frac{R_p}{R_{pI}} = \left(\frac{R_{iI} + R_{iIC}}{R_{iI}}\right)^{0.5} = \left(1 + k' \frac{[\mathrm{C}]}{[\mathrm{BPO}]^{0.5}}\right)^{0.5} \tag{12}$$

$(R_p/R_{pI})^2$ should have a linear relationship with $[\mathrm{C}]/([\mathrm{BPO}]^{0.5})$. Figure 7 shows that $(R_p/R_{pI})^2$ versus $[\mathrm{C}]/([\mathrm{BPO}]^{0.5})$ provides a good linear relationship, and this is quite consistent with the previously proposed mechanism.

GPC results

The obtained nanocomposites with different Cloisite 6A input quantities (the BPO concentration was fixed at 0.005 mol L^{-1}) were exposed to boiling chloroform with a Soxhlet extractor for 50 h to recover the PS macromolecules. The mass weights determined by GPC are listed in Table II. The weight-average molecular weights (M_w's), number-average molecular weights (M_n's), and PDIs of the recovered PS de-

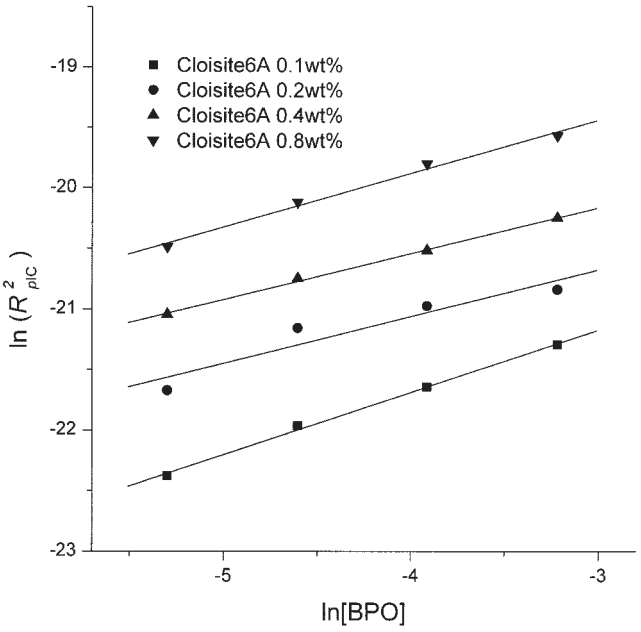

Figure 5 Plots of ln R^2_{pIC} versus ln[BPO].

creased with increasing Cloisite 6A content, and this indicated an increasing radical concentration in the polymerization. This was quite consistent with the results of Laus et al.,[9] who prepared PS/OMMT nanocomposites by emulsion intercalative polymerization.

Under the assumption of bimolecular termination, the kinetic chain length (ν) with different Cloisite 6A input quantities was calculated from M_n as follows:

$$\nu = \frac{M_n}{2} \tag{13}$$

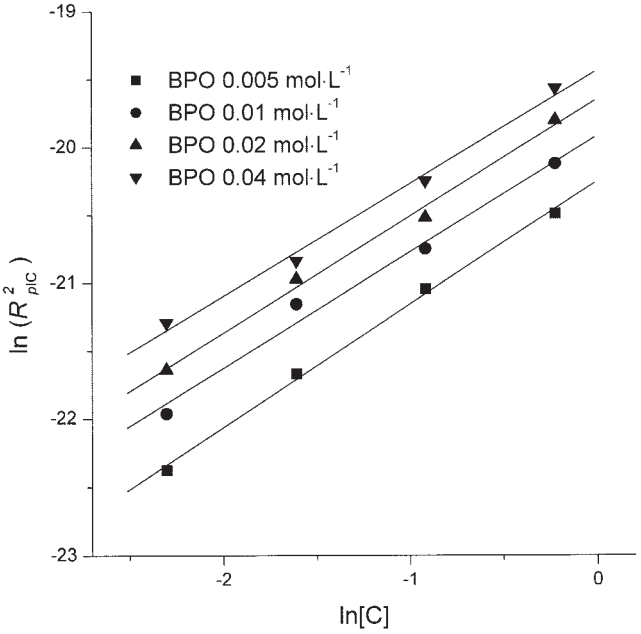

Figure 6 Plots of ln R^2_{pIC} versus ln[C].

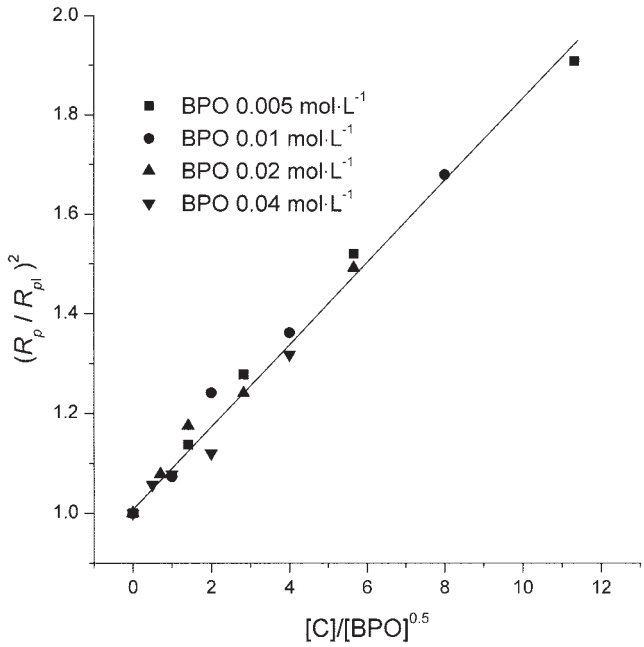

Figure 7 Plots of $(R_p/R_{pI})^2$ versus [C]/([BPO]$^{0.5}$).

Also, the chain initiation rate (R_i) was obtained as follows:

$$R_i = \frac{R_p}{\nu} \tag{14}$$

The obtained results are listed in Table III. The initiation rate increased with an increasing input quantity of clay. Also, R_{iIC} was obtained by the subtraction of R_{iI} from R_i. A plot of ln R_{iIC} versus ln[C] is shown in Figure 8 and yields a slope of 0.886. This is quite consistent with that obtained directly from the polymerization rate data (see Fig. 6).

Structural characterization

XRD patterns of Cloisite 6A and PS/Cloisite 6A nanocomposites prepared with different BPO concentrations (the Cloisite 6A input quantity was fixed at 0.8 wt %) in the range of 2θ = 1–10° are shown in Figure 9. The actual clay contents in the obtained PS/Cloisite

TABLE II
Molecular Weight of PS in the Composites Prepared at Different Cloisite 6A Input Quantities

Cloisite 6A input quantity (wt %)	$M_w \times 10^{-4}$	$M_n \times 10^{-4}$	PDI (M_w/M_n)
0	22.24	8.37	2.66
0.1	21.01	7.69	2.73
0.2	18.06	6.49	2.78
0.4	13.73	6.11	2.25
0.8	13.32	5.56	2.40

TABLE III
R_i Values of the Bulk Polymerization of St with Different Cloisite 6A Input Quantities

	Cloisite 6A input quantity (wt %)				
	0	0.1	0.2	0.4	0.8
R_i (10^{-10} mol L^{-1} s^{-1})	8.82	10.23	12.84	14.87	18.32

6A nanocomposites, estimated from the conversion of monomer St, and the interlayer distances (d_{001}) of the clay, calculated with the Bragg equation ($2d \sin \theta = \lambda$), are listed in Table IV.

When the BPO concentration was 0.04 mol L^{-1}, a strong diffraction peak at 3.70 nm corresponding to the 001 plane could be observed. The increase in d_{001}, with respect to a value of 3.42 nm for Cloisite 6A, was larger than 0.02 nm for the PS/Cloisite 6A nanocomposites prepared by intercalative polymerization and studied by Doh and Cho[10] but was consistent with the results of melt intercalation studied by Lim and Park.[11] This confirmed the intercalative reaction of PS into the clay galleries. A higher order peak corresponding to the 002 plane was also clearly observed, and this suggested that the layer structure was mostly maintained.[12]

The nanocomposites showed remarkably different XRD patterns, although they were prepared under the same conditions, such as the temperature and clay input quantity (the actual clay contents were also little different; see Table IV), except for the different BPO concentrations. The diffraction peak of the 001 plane was extremely weakened with a lower BPO concentration and with a larger value of d_{001}. When the BPO concentration was 0.005 mol L^{-1}, d_{001} was calculated to be 3.87 nm, and the diffraction peak was very inconspicuous. This suggested that the layer structure of the clay was largely destroyed. This result was consistent with our previous study of PMMA/OMMT nanocomposites.[5]

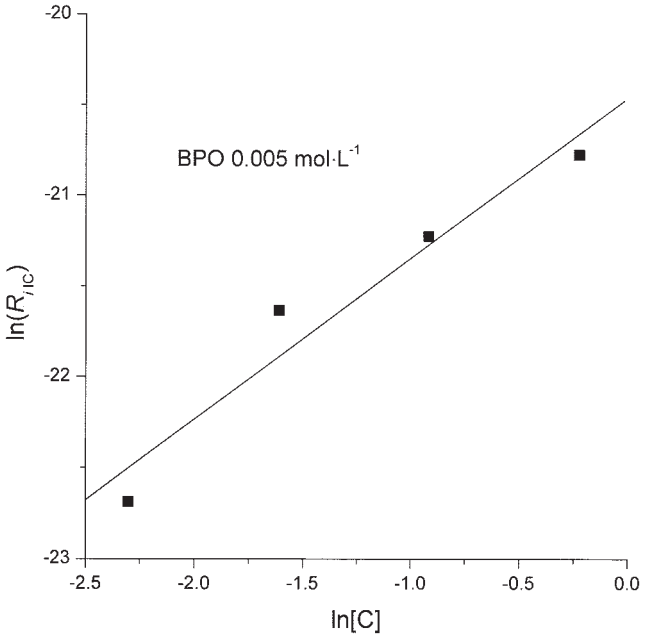

Figure 8 Plots of ln R_{iIC} versus ln[C].

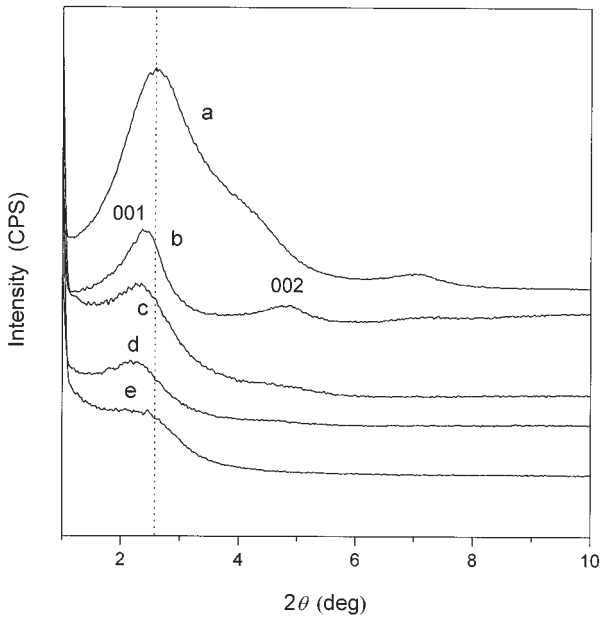

Figure 9 XRD patterns of (a) Cloisite 6A and (b–e) PS/Cloisite A nanocomposites prepared at BPO concentrations of 0.04, 0.02, 0.01, and 0.005 mol L^{-1}, respectively.

The change in the XRD patterns indicated that the layer structure was not by any means the same when the Cloisite 6A input quantity and the polymerization conditions were fixed. It was also affected by the concentration of the initiator. Although the mass weight of PS was affected by the BPO concentration, studies showed that the mass weight of the macromolecules had no effect on the interlayer distance.[13] On the contrary, a higher molecular weight reduced the intercalative rate of the polymer chain into the interspacing of the clay. According to the mechanism proposed in this article, a lower initiator concentration caused an increased amount of Cloisite 6A to participate in the chain initiation. Then, more clay was interacted with the PS macromolecules, and this in turn caused more

TABLE IV
d_{001} Values of PS/Clay Nanocomposites Prepared with Different BPO Concentrations

	Cloisite 6A	[BPO] (mol/L)			
		0.04	0.02	0.01	0.005
Clay content (wt %)	100	12.65	14.31	14.07	13.84
d_{001} (nm)	3.42	3.70	3.84	4.09	3.98
Δd (nm)	—	0.28	0.42	0.67	0.56

Δd = increase in interlayer distance.

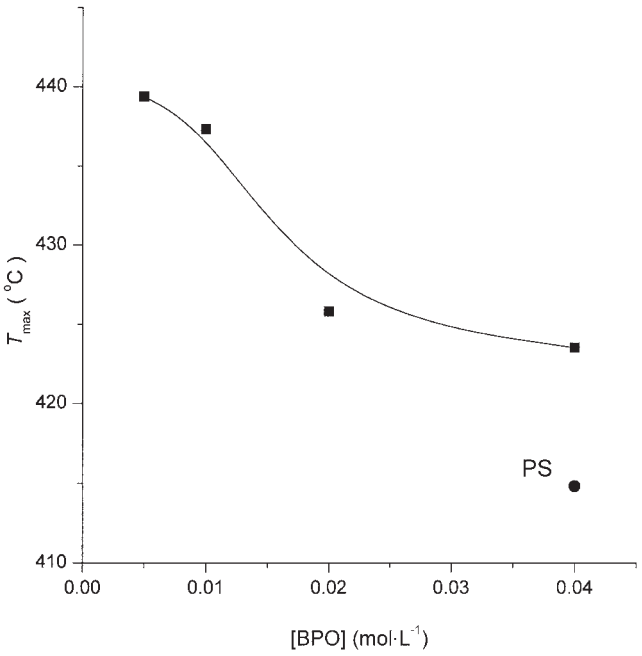

Figure 10 T_{max} of PS/Cloisite 6A nanocomposites prepared at different BPO concentrations.

of the layer structure to be destroyed. This is the reason that the delamination of the clay layer increased with decreasing BPO concentration. Dekking[14] prepared PMMA/bentonite intercalative composites with kaolin as the adduct and with 2,2′-azobisisobutyramidine hydrochloride as the initiator. The extraction results showed that increasing the accessibility of the monomer to the clay increased the quantity of the nonextractable polymer in the composites. This meant that the interaction of the polymer with the clay layer was enforced if the clay participated in the initiation of the chain, and this was also the case in our experiments.

Thermal properties

T_{max} of the aforementioned nanocomposites is shown in Figure 10. At a higher BPO concentration, a lower value of T_{max} was observed, and this was due to the higher order of the layer structure of the clay. Chen et al.[15] showed that the higher decomposition temperature of the PCN nanocomposites could be attributed to the nanoscale clay sheets preventing the out-diffusion of the volatile decomposition products. Therefore, the nanocomposites prepared with lower BPO concentrations, which had higher dispersability of clay in the polymer matrix, greatly increased the distance of the pathways of the volatile decomposition products and had higher heat-decomposition-resistance temperatures.

CONCLUSIONS

The bulk polymerization rates of St increased remarkably in the presence of the MMT Cloisite 6A. Cloisite 6A participated in the radical initiation reaction of the radical, and the reaction orders with respect to the clay and BPO were approximately 1.0 and 0.5, respectively. The layer structure of the clay in the PS/Cloisite 6A nanocomposites prepared with lower BPO concentrations was destroyed more than the layer structure in the nanocomposites prepared with higher BPO concentrations. At the same time, the nanocomposites prepared with lower BPO concentrations had higher heat-decomposition-resistance temperatures.

References

1. Shi, H.; Lan, T.; Pinnavaia, T. J. Chem Mater 1996, 8, 1584.
2. Ballantine, J. A.; Davies, K. J.; Purnell, J. H.; Rayanakorn, M.; Thomas, J. M.; Williams, K. J. J Mol Catal 1984, 26, 37.
3. Uskov, I. A. High Mol Weight Compd 1960, 6, 926.
4. Al-Esaimi, M. M. J Appl Polym Sci 1997, 64, 367.
5. Liu, G. D.; Zhang, L. C.; Qu, X. W.; Wang, B. T.; Zhang, Y. J Appl Polym Sci 2003, 90, 3690.
6. Solomon, D. H.; Swift, J. D. J Appl Polym Sci 1967, 11, 2567.
7. Pan, Z. R. Polymer Chemistry; Chemical Industry: Beijing; 1997.
8. Shan, G. R.; Huang, Z. M.; Weng, Z. X.; Pan, Z. R. Macromolecules 1997, 30, 1279.
9. Laus, M.; Camerani, M.; Lelli, M.; Sparnacci, K.; Sandrolini, F. J Mater Sci 1998, 33, 2883.
10. Doh, J. G.; Cho, I. Polym Bull 1998, 41, 511.
11. Lim, Y. T.; Park, O. O. Macromol Rapid Commun 2000, 21, 231.
12. Vaia, R. A.; Giannelis, E. P. Macromolecules 1997, 30, 8000.
13. Vaia, R. A.; Ishii, H.; Giannelis, E. P. Chem Mater 1993, 5, 1694.
14. Dekking, H. G. G. J Appl Polym Sci 1967, 11, 23.
15. Chen, G. M.; Liu, S. H.; Chen, S. J.; Qi, Z. N. Macromol Chem Phys 2001, 202, 1189.